VSP azimuthal travel time analysis at the Field Research Station near Brooks, Alberta

Adriana Gordon, Don C. Lawton and David W. Eaton

ABSTRACT

As part of the Containment and Monitoring Institute (CaMI) CO_2 injection project, Vertical Seismic Profile data (VSP) were acquired at the Field Research Station in May 2015. A half walk-around VSP survey was acquired and processed for an azimuthal analysis. Obtaining the first break traveltime variations with azimuth, was the first step. Statics corrections and median filters were applied to help differentiate a sinusoidal trend in the data. The fast direction, estimated from the trend, is at approximately 40 degrees, which is similar to the Western Canada stress orientation (NE-SW). An estimation of the anisotropy parameter epsilon (ε) yield a value of 0.02, indicative of weak anisotropy. The data was rotated as a starting point of the processing flow by using with different approaches, in order to obtain imaging results in the future work. However, further analysis must be done in order to obtain a more detailed conclusion.

INTRODUCTION

The Containment and Monitoring Institute (CaMI) is developing a Field Research Station (FRS) in junction with the University of Calgary. The objective of FRS is to facilitate and to accelerate research and development leading to improved understandings and technologies for geological containment and storage of CO_2, monitoring of fossil fuel production, and environmental mitigation (Lawton et. al., 2014).

The purpose of this project is to identify azimuthal anisotropy at the Field Research Station (FRS) in order to characterize the study area where the CO_2 injection will take place. Therefore, the velocity changes will be analyzed by processing the half walk-around vertical seismic profile (VSP) data acquired on May 2015.

The next part of this work is rotate the half walk-around VSP data, been the first step of the processing flow. The horizontal components H1 and H2 are rotated in the Hmax and Hmin direction. The vertical component Z and Hmax are rotated in the Hmax' and Z' direction, in order to have the data oriented in the radial, transverse and vertical coordinate system. The results of the second rotation are also compared with the incidence angle calculated with a ray-tracing computation of a velocity model created from a sonic log.

THEORY

Anisotropy

Anisotropy can be defined as the variation of a material's property with respect to the direction in which it is measured. Rock formations can be anisotropic in terms of a variety of measurements, including resistivity, permeability, and elastic properties. Because seismic wave propagation is controlled by the elastic properties of a material, materials with elastic anisotropy exhibit directional variations in the speed of waves travelling through the material (Evans et. al., 2010).

In 1986, Thomsen stated that the simplest anisotropic case of broad geophysical applicability has one distinct direction (usually, but not always, vertical), while the other two directions are equivalent to each other. This case is called transverse isotropy (TI) or hexagonal symmetry. By focusing in a vertical symmetry axis, Thomsen defined three anisotropy parameters (ε, γ and δ) from the elastic modulus tensor. These parameters should be appropriate combinations of elastic moduli, they are nondimensional, so that one may speak of X percent of P anisotropy; and reduce to zero in the degenerate case of isotropy, so that materials with small values ($\ll 1$) of "anisotropy" may be denoted "weakly anisotropy" (Thomsen, 1986).

As mentioned above, one of the most common causes of elastic anisotropy is layering. Horizontal layers may have isotropic elastic properties that differ between layers, or they may be anisotropic themselves. When this stack of layers is probed with seismic waves of wavelength larger that the individual layers, the result is an averaged, or effective, response that depends on direction. Such media are said to have vertical transverse isotropy (VTI) (Evans et. al., 2010).

Another important case of transverse isotropy is represented by horizontal transverse isotropy or HTI media, where the symmetry axis lies in the horizontal plane. Materials containing aligned vertical fractures or cracks that are rotationally invariant about their normal exhibit HTI symmetry. The strike of open vertical fractures or cracks at depth can often be related to the direction of maximum horizontal compressive stress (Liu et. al., 2012).

Thomsen defined the anisotropy parameter epsilon as the fractional difference between vertical and horizontal P velocities (Equation 1)

$$\varepsilon = \frac{v_p\left(\frac{\pi}{2}\right) - \alpha_0}{\alpha_0}, \tag{1}$$

where α_0 is the vertical P velocity and $v_p\left(\frac{\pi}{2}\right)$ is the horizontal P velocity. Taking in consideration that the focus of his work was VTI media, and for that case the fast direction is horizontal and the slow direction is vertical, Equation 1 can be described as the fractional difference between the fast and slow velocities (Equation 2),

$$\varepsilon = \frac{v_{fast} - v_{slow}}{v_{slow}}. \tag{2}$$

VTI and HTI symmetry are also referred to as polar anisotropy and azimuthal anisotropy, respectively. A common cause of this form of anisotropy in sedimentary basins is a combination of thin layering and vertical aligned fractures (Liu et. al., 2012).

Some of the major applications of seismic anisotropy involve improving seismic imaging, improving seismic-well ties, AVO analysis, and fracture detection using azimuthal anisotropy (Liu et. al., 2012). In this case, our focus is to identify azimuthal anisotropy and in order to find evidence of this type of anisotropy, hence a walk-around VSP survey was acquired on May 2015.

Vertical Seismic Profile (VSP)

A vertical seismic profile (VSP) is a measurement procedure in which a seismic signal generated at the surface of the earth is recorded by geophones secured at various depths to the wall of a drilled well (Hardage, 2000). Vertical seismic profile (VSP) surveys differ from other types of borehole and surface seismic methods in that they utilize surface sources and borehole receivers to record both upgoing and downgoing wavefields. Strong and consistent sources are available for use on or near the surface, and the borehole provides a relatively noise-free environment for VSP recording (Hinds et. al., 1996).

The conventional VSP, with an array of geophones along the borehole and the source on the surface, is the most familiar example; but the variety of possible arrangements, borehole orientations, and objectives is much wider than this. The term zero-offset VSP refers to a geometrical configuration where the source and receiver locations are vertically aligned, or can be treated as such during processing. The offset VSP refers to a geometrical configuration where the source and receiver locations cannot be treated as vertically aligned during processing. The walk-away VSP configuration is similar to the offset VSP because the sources are placed at increasing distances from the well, while the receivers remain in the wellbore. In walk-around surveys, offset source locations span a large circular arc to probe the formation from a wide range of azimuths (Evans et. al., 2010; Hinds et. al., 1996).

Hodogram analysis

In a 3C VSP survey, at any given tool location, three channels of data are recorded (Z, X and Y) where X and Y record data from the two horizontal geophones (Hinds et. al., 1996). The orientation of the horizontal geophones in the wellbore is normally unknown and will generally vary between tool positions as the tool rotates on the end of the wireline cable (Evans et. al., 2010). Therefore, the processing of the 3C walk-around VSP data includes geophone orientation estimation using P-wave hodogram analysis. Once the geophone orientation has been estimated, the data are rotated into the radial, transverse and vertical coordinate system for each of the shot positions (Horne et. al., 2000).

Hodogram analysis performed on the first-break wavelets of the two horizontal datasets is used to polarize X and Y data onto two principal axes that are normal (Hmin) and tangential (Hmax) to the plane defined by the source and the well (Hinds et. al., 1996).

The hodogram is constructed using a window of data around the first-break wavelet, in this case the window length used was of 100ms. This is done interactively using a color-coded display that enables the interpreter/processor to understand what part of the hodogram relates to individual portions of the windowed data. The angle used in the rotation matrix is chosen calculating a line through the hodogram display that can be rotated interactively, plus the output data window is redisplayed each time the line is rotated (Hinds et. al., 1996).

DATA SET AND SOFTWARE

In May of 2015 a 2D Surface Seismic and a 3C walk-away and half walk-around Vertical Seismic Profile (VSP) survey was recorded at the FRS with the collaboration of the Microseismic Industry Consortium. The area of study is located in southern Alberta, approximately 189 km southeast of Calgary and 25 km southwest of Brooks (Figure 1).

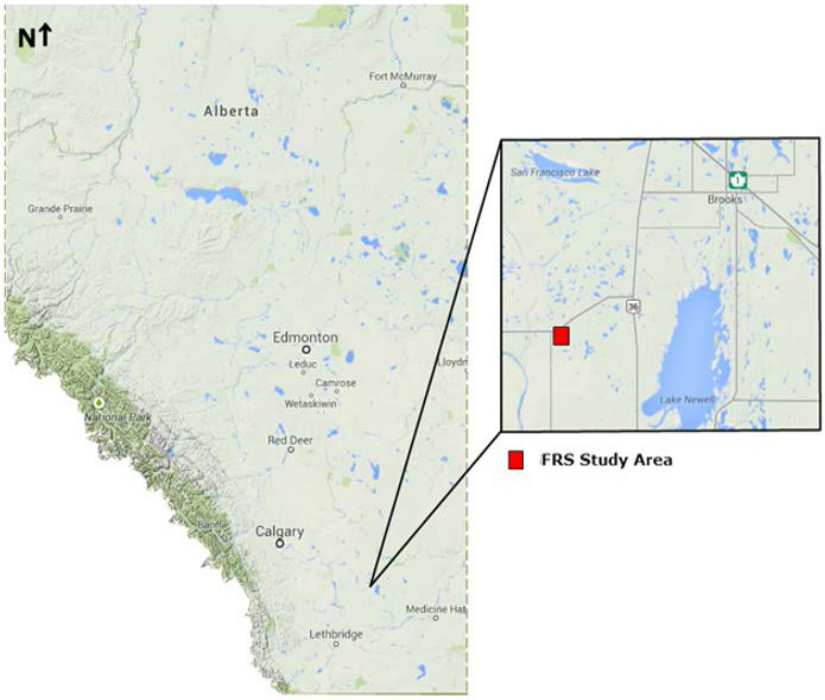

FIG. 1. FRS location. Modified from Dongas et. al., 2014.

The acquisition design for the VSP surveys as illustrated in Figure 2; centered on the well CMCRI COUNTESS 10-22-17-16. A three-component ESG SuperCable was deployed in the well at three different levels, giving receiver positions in the well ranging from 106 to 496 meters depth at 15 m spacing. The source was an IVI EnviroVibe, sweeping from 10-200 Hz linearly over 16 seconds with an additional 4 seconds listening time. Two source lines were acquired three times, once for each tool position in the well. Source line 208 (NE-SW) had 10 m Vibe Points (VP), offset NW of the surface receiver locations, for a walkaway VSP. A semi-circular source line (204) with a radius of 400 m and a VP every five degrees was acquired for a velocity tomography study and an azimuthal analysis (Hall et. al., 2015).

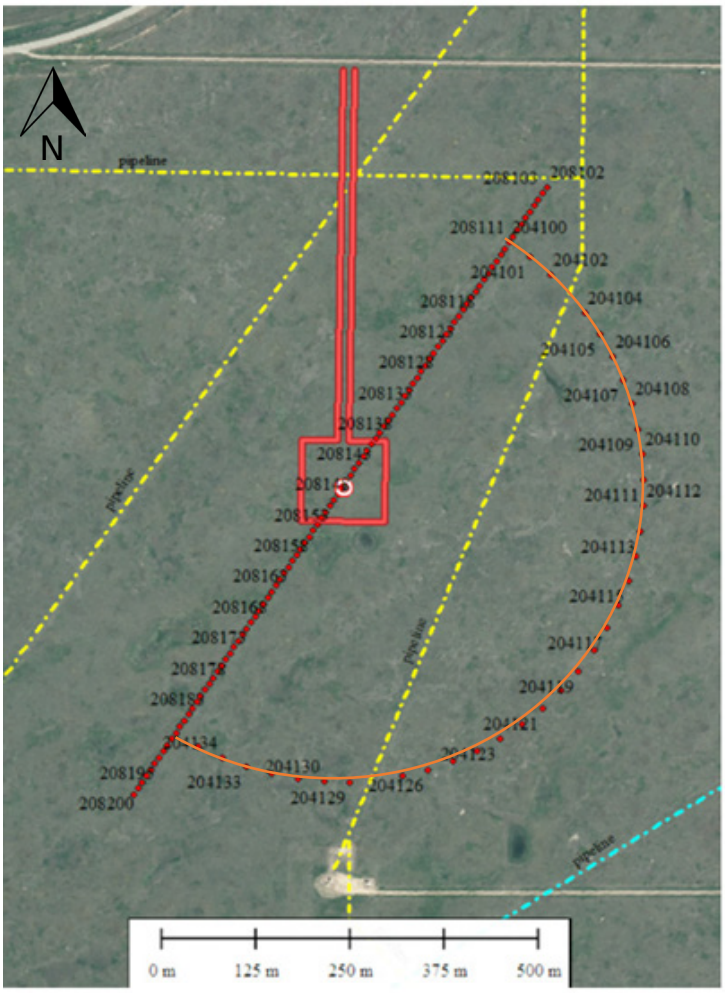

FIG. 2. Acquisition design. Source lines 208 and 204 (red dots and orange line). Buried pipelines are plotted as yellow/cyan dash-dot lines. The access road and well pad are shown as solid red lines, and the well location is a red bulls-eye. Modified from Hall et al., 2015.

During this project, VISTA Desktop Seismic Data Processing Software provided by Schlumberger was used for processing the data. Also, the software MATLAB by MathWorks (including CREWES toolbox) was used in different parts of this research to obtain a better understanding on the processing work flow.

PROCEDURE AND RESULTS

The first step in VSP processing, was to set up the geometry. Figure 3 represents the geometry of the walk-around VSP data uploaded to VISTA, where the receivers are in green, and the shots are in black and red. The next step was the first break picking of the vertical component of the zero offset VSP in this case, the shot 126 of the walk-away VSP (Line 208); and the first break picking for all the shots of line 204 (walk-around VSP). An example of the first break picking of the zero offset VSP is shown in Figure 4. Notice that the second trace started recording earlier that the rest, this may be due to an inconsistency between the time on the receiver and the GPS used during the recording. Data from this geophone were not used in the analysis.

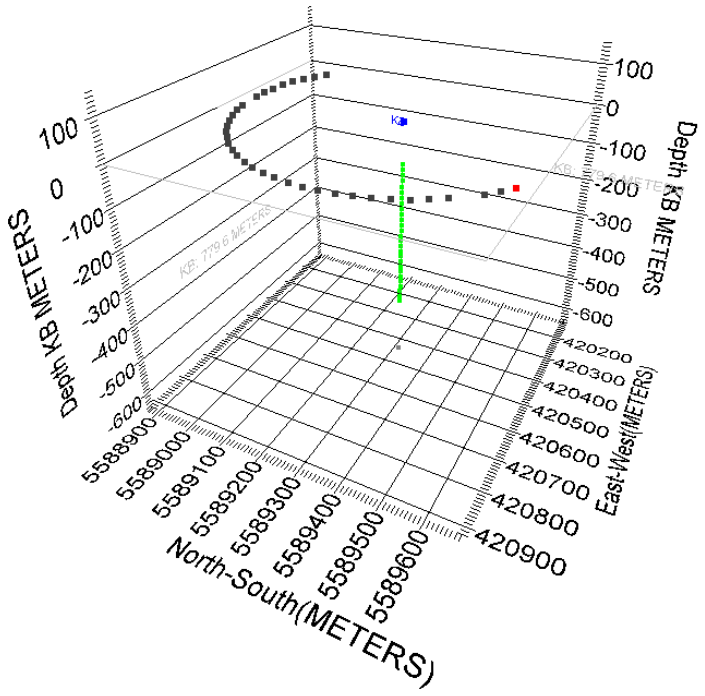

FIG. 3. Walk-around VSP geometry (Line 204). Black dots represent the sources, green dots represent the receivers, the red point marks an arbitrary shot and the blue point shows the wellbore on surface.

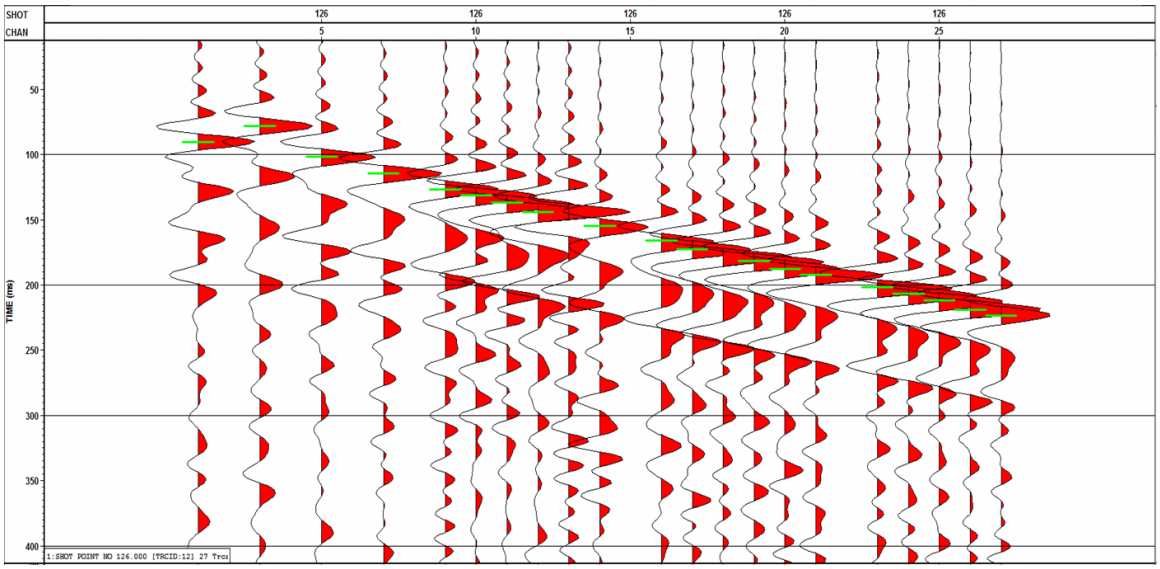

FIG. 4. First break picks in green of the zero-offset VSP, vertical component (line 208, shot 126).

First break traveltime variation with azimuth

In order to undertake azimuth velocity analysis, the first break traveltimes of the walk-around VSP (Line 204) were plotted for each receiver as a function of azimuth. By sorting seismic data into azimuthal gathers, a sinusoidal variation in traveltime with azimuth would

generally indicate the presence of azimuthal anisotropy (HTI) (Liu et. al., 2012). Due to the regional stress field of the study area, the possibility of fractures is not unlikely. Since the acquisition configuration for the walk-around is a semi-circle instead of a complete circle, we would expect a half period sinusoidal traveltime variation. This plot was created in MATLAB, after exporting the first break picks from VISTA. One remark about this graph is the high precision of the first break picks for all the receivers, almost each point is in resonance with the general trend. However, the graph has a considerable amount of noise and therefore a statics correction was applied.

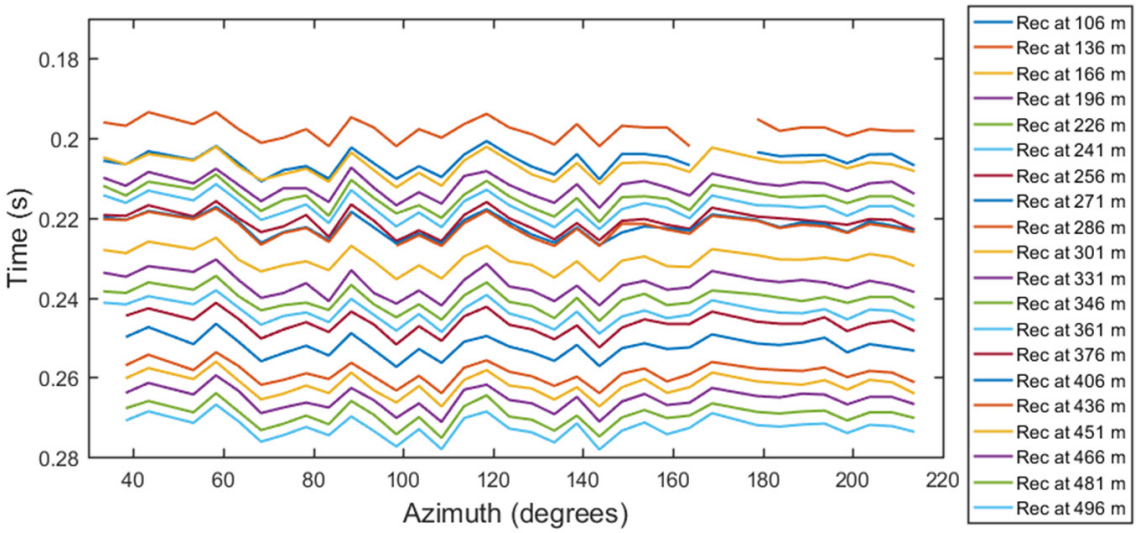

FIG. 5. First break picks versus azimuth for each receiver of line 204. Each colored curve represents a receiver depth.

Statics correction

The shot statics from the 3D seismic survey in the study area were used to apply the static corrections to the observed traveltimes. The variations may be associated with the near-surface layer and not to topography, since the FRS is located in a generally flat area. With the use of MATLAB, all the shot statics around the study area were interpolated and plotted to create a contour map of the shot statics. The shots of the walk-away VSP and walk-around VSP were superimposed over the contour map. All the static values for each shot of the walk-away VSP and walk-around VSP were exported to a text file. Notice that the contour map was smoothed in order to reduce the sharp contour lines due to the interpolation, however the values used for the statics correction were unsmoothed. Figure 6 represents the contour map of the shot statics. Then, the text file containing the shot statics for the walk-away VSP and walk-around VSP was imported to VISTA. Once the correction was made, the plot of the first break traveltimes versus azimuth was edited and some missing points were extrapolated. The result is shown in Figure 7. Since the values of the shot statics were considerable small, noise is still present. However, some small variations are visible after correction, as on the edges of the chart where the curves have a flatter and steadier appearance.

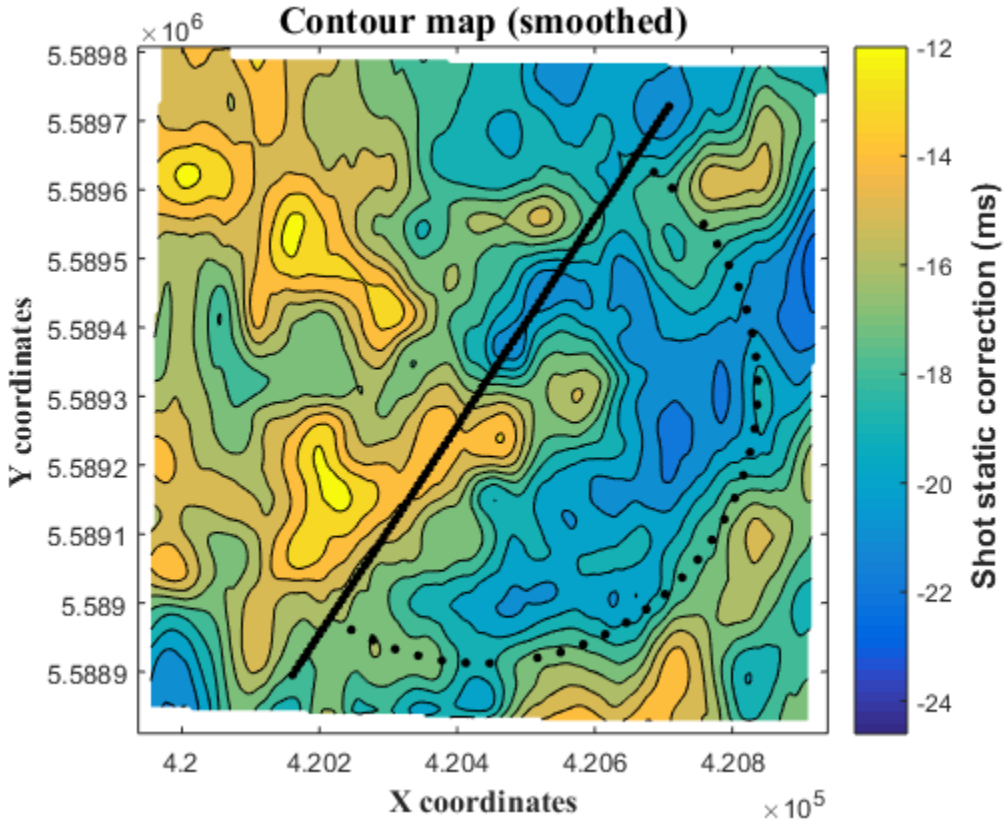

FIG. 6. Shot statics contour map.

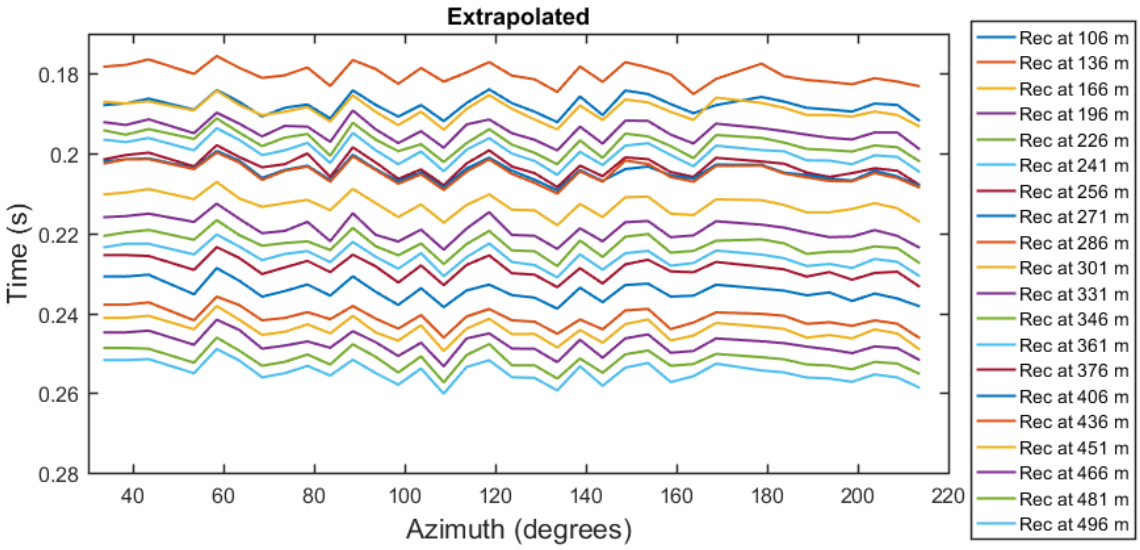

FIG. 7. First break picks versus azimuth for each receiver of shot line 204 after static correction. Each colored curve represents a receiver depth.

Several median filters were applied to the plot on Figure 7 in order to smooth the data present in the charts. Figure 8 shows the graph obtained after a median filter of 7 samples was applied. With this filter the noise trend is attenuated and a flatter shape is observed.

Also, a subtle traveltime increase in the center of the plot is noticeable which appears to fluctuate as the azimuth increases. This may be an indicative of a sinusoidal shape.

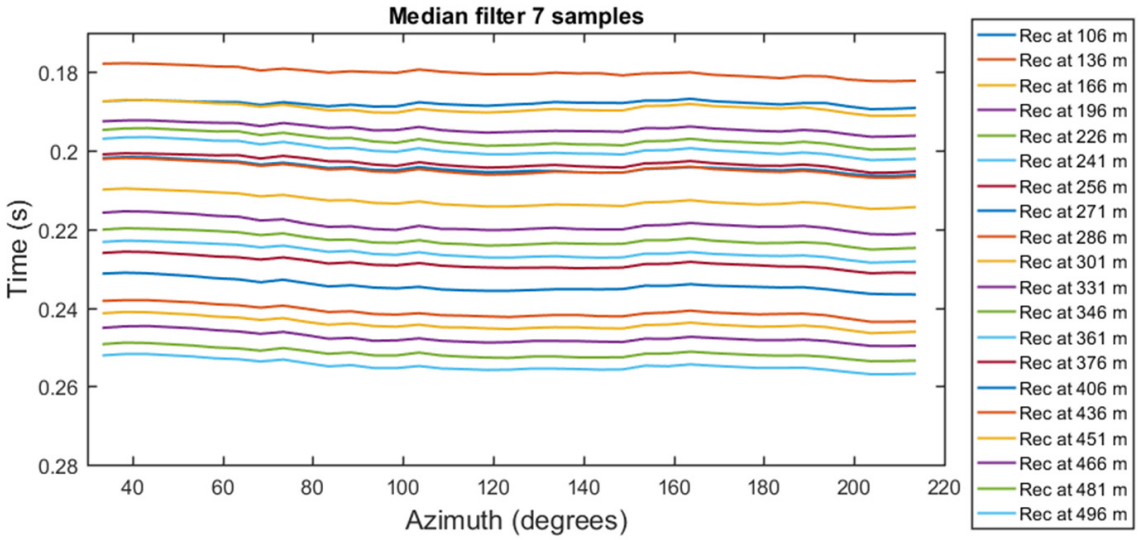

FIG. 8. First break picks versus azimuth for each receiver of shot line 204 after static corrections and median filter of 7 samples. Each colored curve represents a receiver depth.

By reviewing the data at a larger scale it is possible to distinguish a sinusoidal trend more clearly, as shown in Figure 9. From this result, we could state that the fast direction is around a 40-degrees azimuth which has a similarity with the stress orientation in Western Canada (NE-SW).

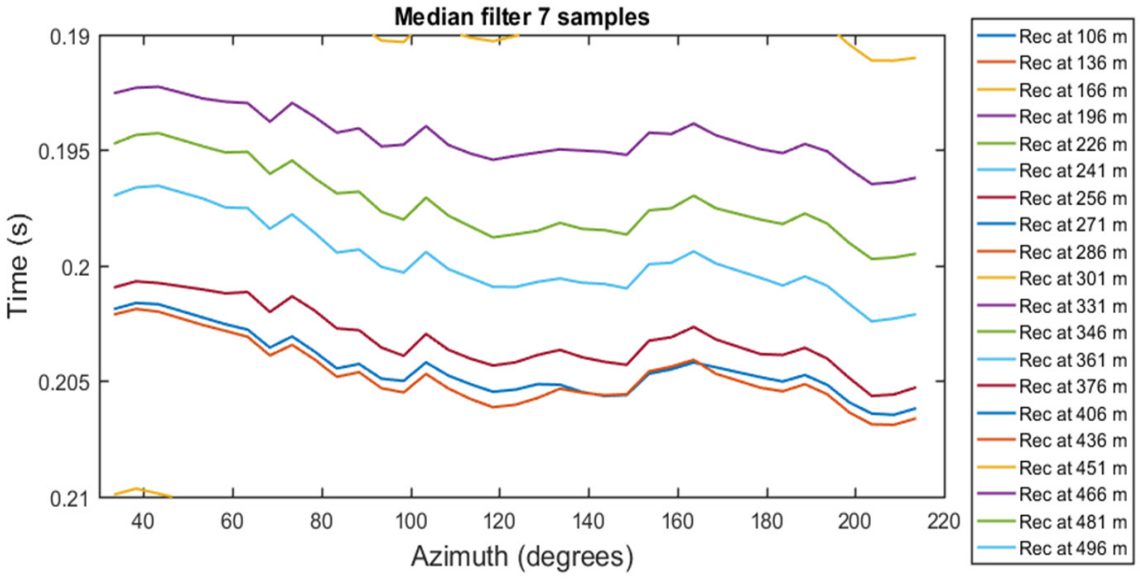

FIG. 9. First break picks versus azimuth for each receiver of shot line 204 after static corrections and median filter of 7 samples using a larger scale. Each colored curve represents a receiver depth.

Estimation of the anisotropy parameter epsilon (ε)

The following step was a residual estimation. This was done by fitting different polynomial equations of different orders to the data in a least-squares sense. This estimation was done for the 1st and 3rd order polynomials at three receiver locations (shallow, middle and deep). Figures 10-15 represents the residual calculation in time and velocity, showing, in the first plot the fitting lines overlain on the data, and the residuals obtained from each fitting line in the second plot. As we can see, the 3rd order approaches better to the data, and the residual values range from -2 to 2 milliseconds and -20 to 20 m/s, respectively. From the velocity variations, we were able to estimate the anisotropy parameter epsilon by using Equation 2. This calculation was done for the same three receivers locations. The average result obtained was 0.0198. This small value of epsilon is indicative of weak anisotropy. The residual estimation could be associated to a mathematical equation with the attempt to estimate anisotropy parameters. Thus, additional research is being examined to develop this initiative.

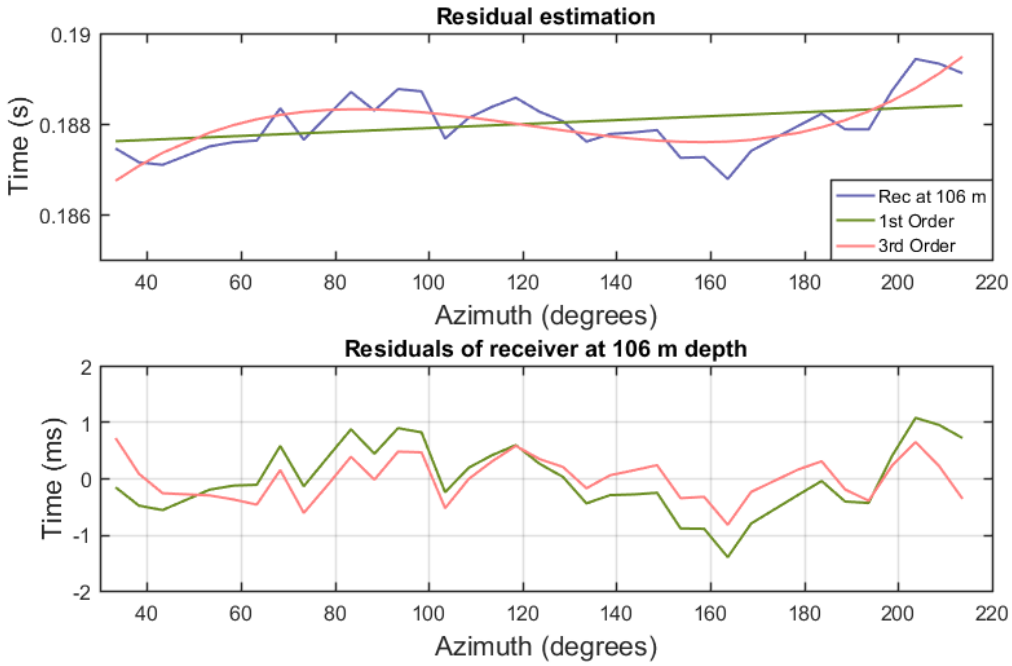

FIG. 10. Traveltime residual estimation of receiver at 106 m depth. Residuals obtained by fitting lines of 1st and 3rd order polynomial (in green and pink respectively) to the data.

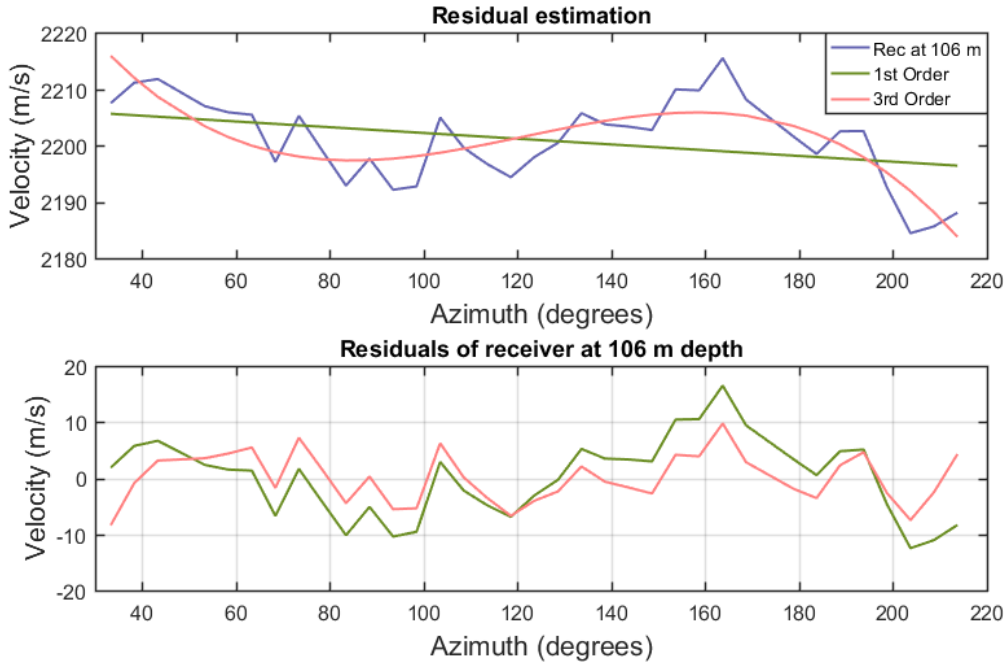

FIG. 11. Velocity residual estimation of receiver at 106 m depth. Residuals obtained by fitting lines of 1st and 3rd order polynomial (in green and pink respectively) to the data.

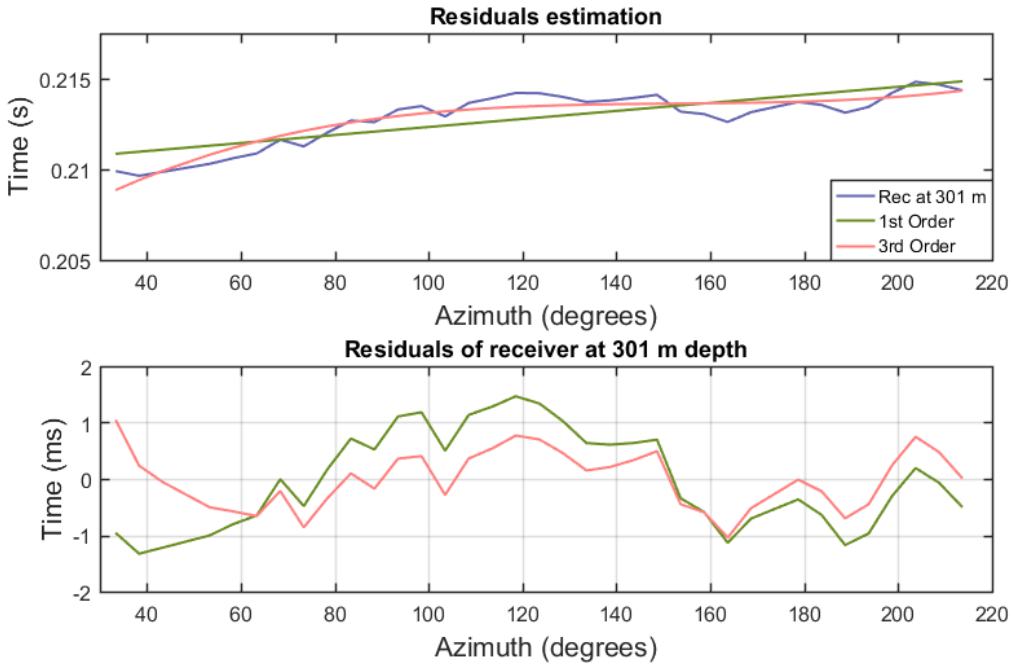

FIG. 12. Traveltime residual estimation of receiver at 301 m depth. Residuals obtained by fitting lines of 1st and 3rd order polynomial (in green and pink respectively) to the data.

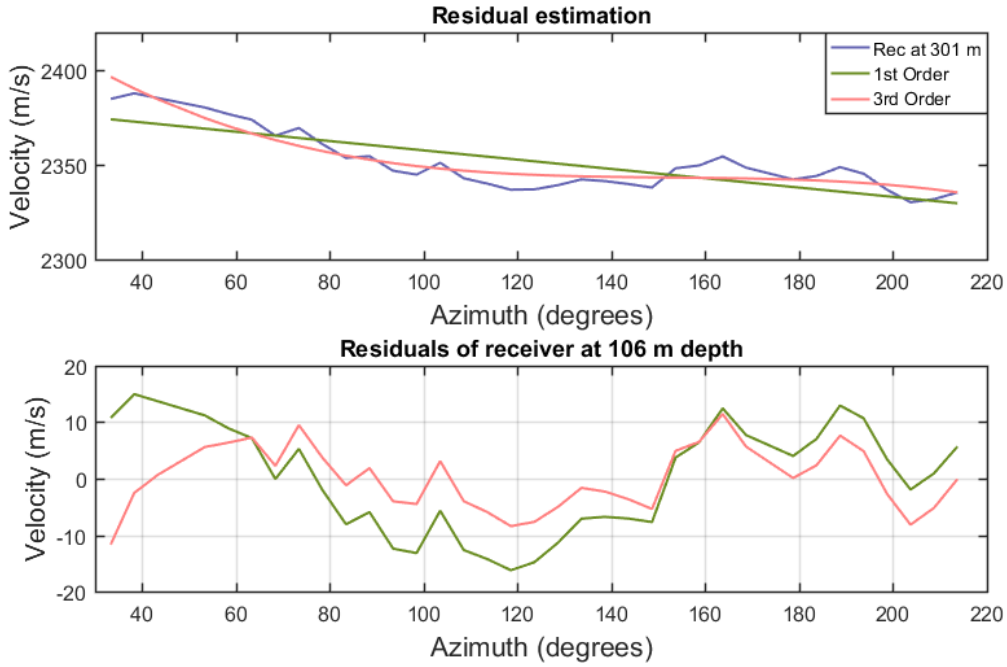

FIG. 13. Velocity residual estimation of receiver at 301 m depth. Residuals obtained by fitting lines of 1st and 3rd order polynomial (in green and pink respectively) to the data.

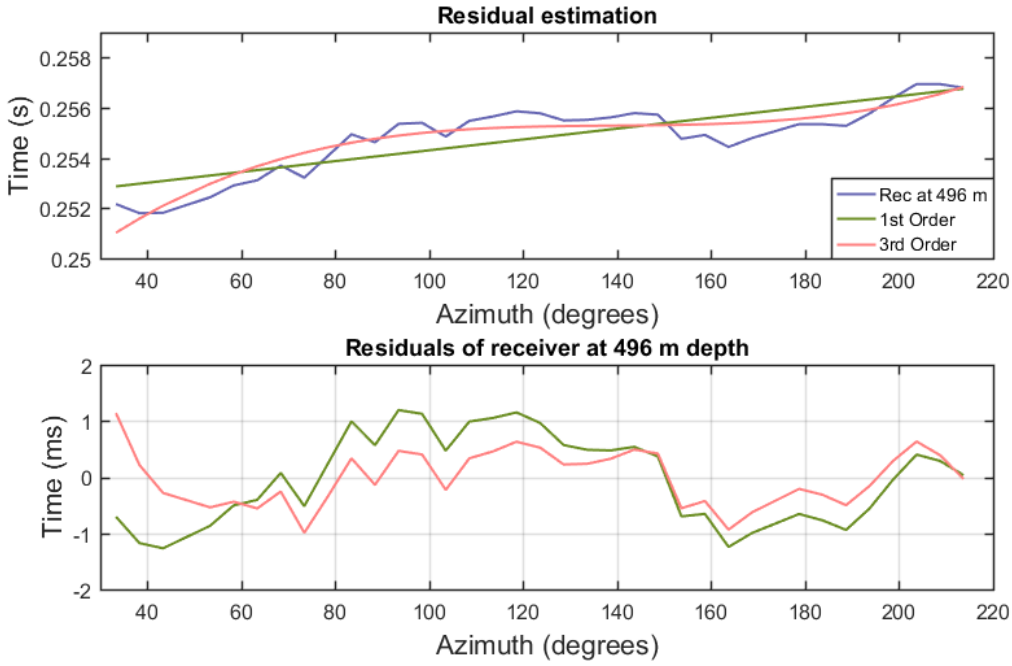

FIG. 14. Traveltime residual estimation of receiver at 496 m depth. Residuals obtained by fitting lines of 1st and 3rd order polynomial (in green and pink respectively) to the data.

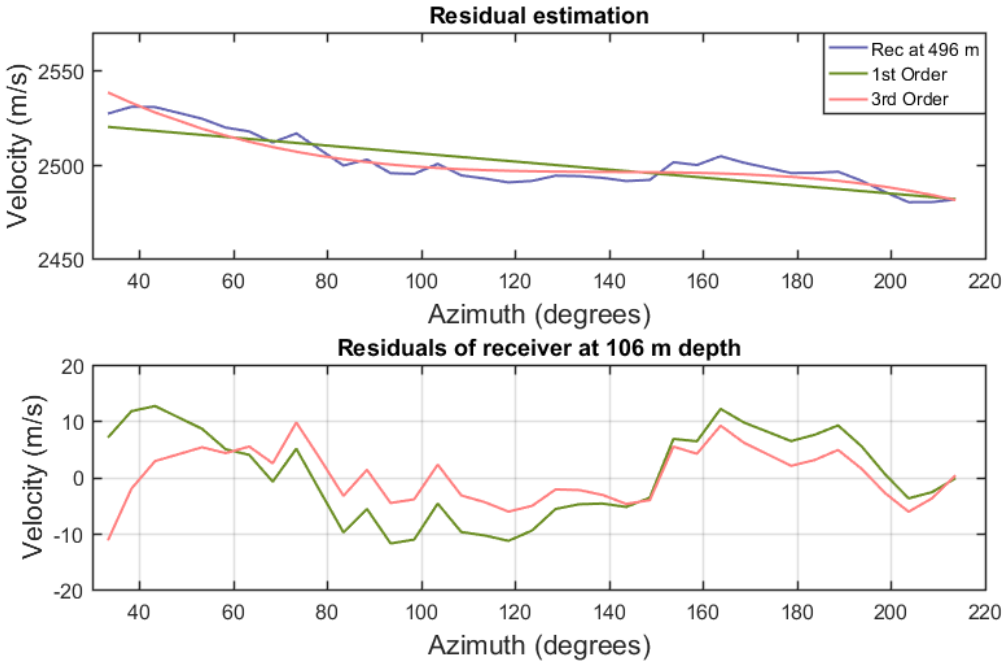

FIG. 15. Velocity residual estimation of receiver at 496 m depth. Residuals obtained by fitting lines of 1st and 3rd order polynomial (in green and pink respectively) to the data.

VSP data rotation

First data rotation

In order to get a better understanding of the VSP data rotation mentioned above, the hodogram analysis was done with two different software. Once using VISTA and a second time coding a script in MATLAB. The results of the two approaches are shown in a crossplot (Figure 16) for three different shots (1, 20 and 30). Also, Figure 17 represents a schematic plan view of the shots selected for this analysis. An accurate relation between the results from VISTA and MATLAB is noticeable. Nevertheless, there are several outliers in Figure 16 that could be associated to the difficulty of identifying first arrivals in the horizontal components of the traces.

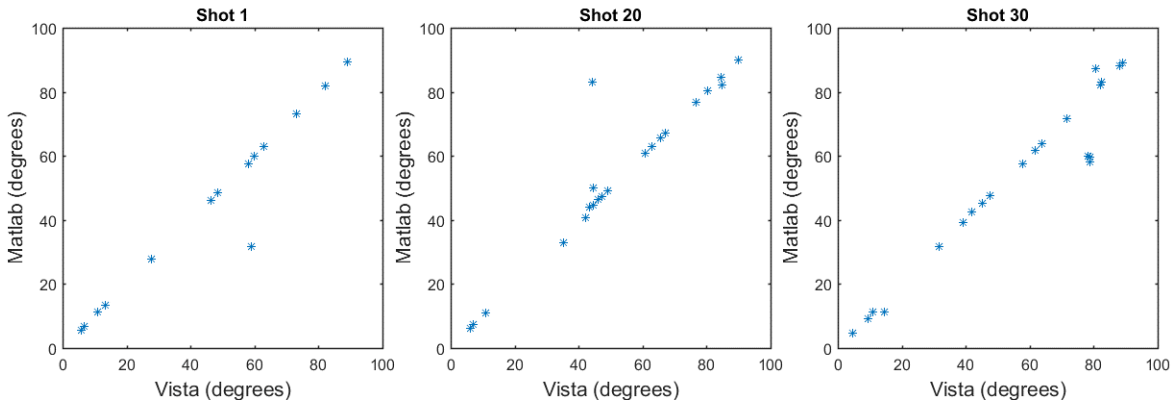

FIG. 16. Crossplot of rotation angles obtained in VISTA and MATLAB for the shots 1, 20 and 30.

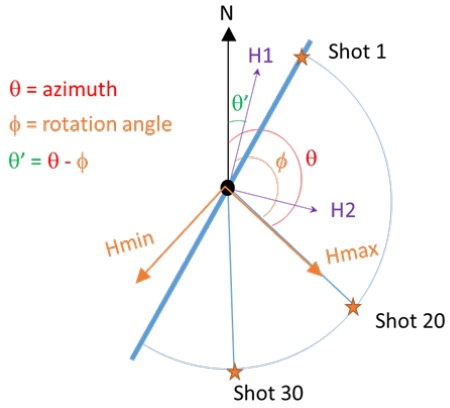

FIG. 17. Schematic plan view of shots 1, 20 and 30 represented by star symbols. The semi-circle blue line represents the VSP geometry and the wellbore head is represented in black.

As mentioned before, since the SuperCable was deployed in the well at three different levels, the difference between the azimuth of the shot and the rotation angle of the horizontal components at each level should have a similar value. By calculating the difference between the azimuth and rotation angle, it is possible to estimate the orientation of the geophones as the super cable was moved inside the borehole. Figure 18 and Figure 19 shows the superposition of the receiver depth vs azimuth for the shots 1, 20 and 30 for the results in VISTA and MATLAB respectively. As expected, the receivers have a similar orientation but there are small variations that need further investigation to ensure that the receivers in the tool are not rotating after being deployed in the well. Figures 20 and 21 shows an example of the data after the rotation. Figure 20 represents the Hmax component and Figure 21 represents the Hmin component. Notice how the amplitude of the first arrivals is stronger in Hmax compared to Hmin, which is expected, transferring the energy from the H1 and H2 components to a maximum and minimum component.

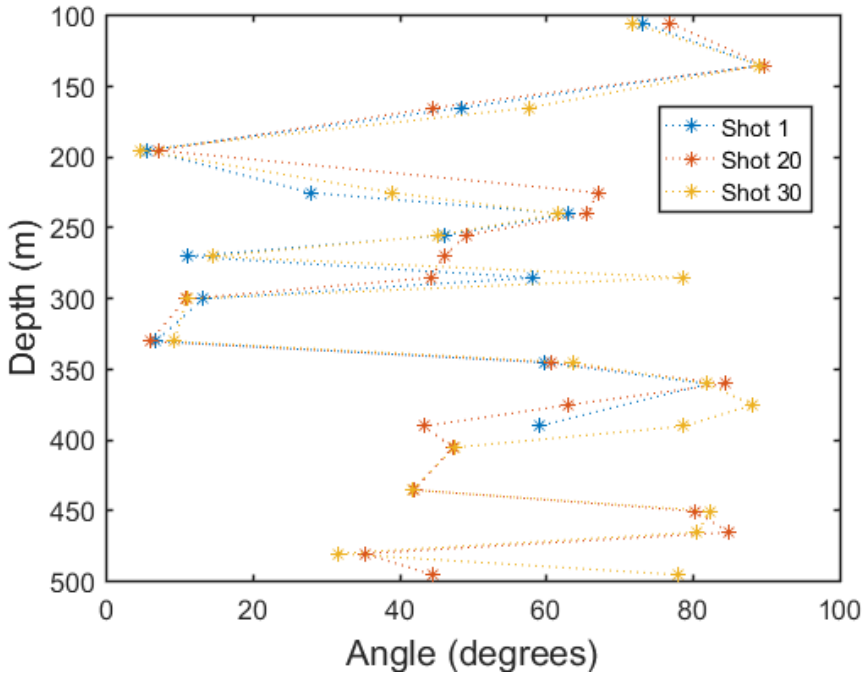

FIG. 18. Receiver depth vs azimuth for the shots 1, 20 and 30, using the results obtained from VISTA.

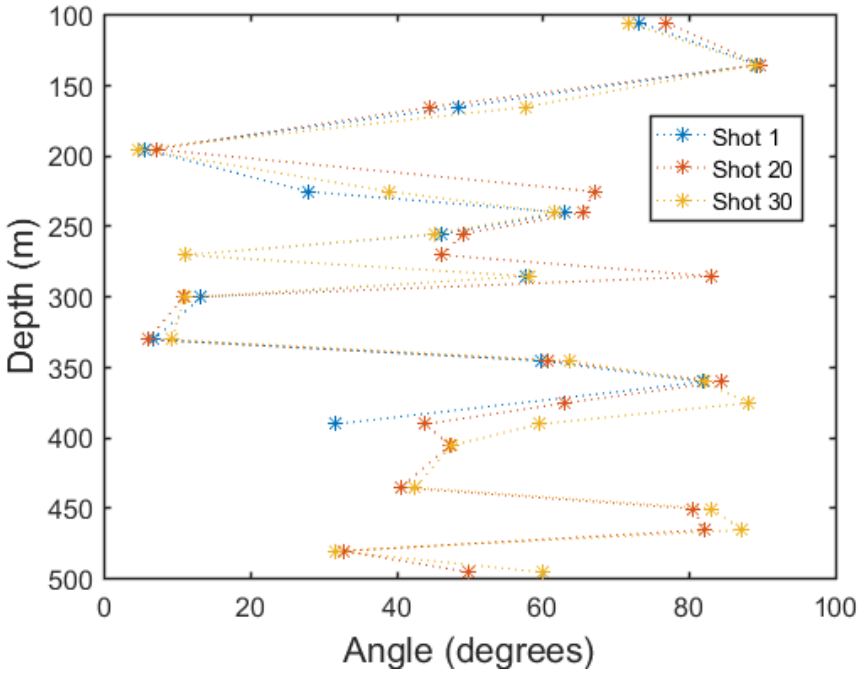

FIG. 19. Receiver depth vs azimuth for the shots 1, 20 and 30, using the results obtained from MATLAB.

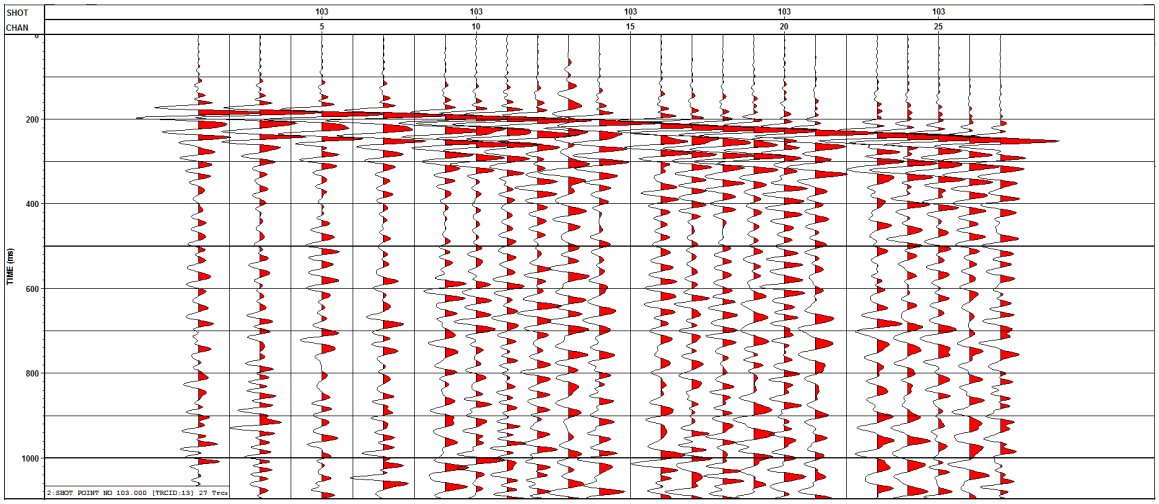

FIG. 20. Example of the Hmax component after first rotation (line 204, shot 103).

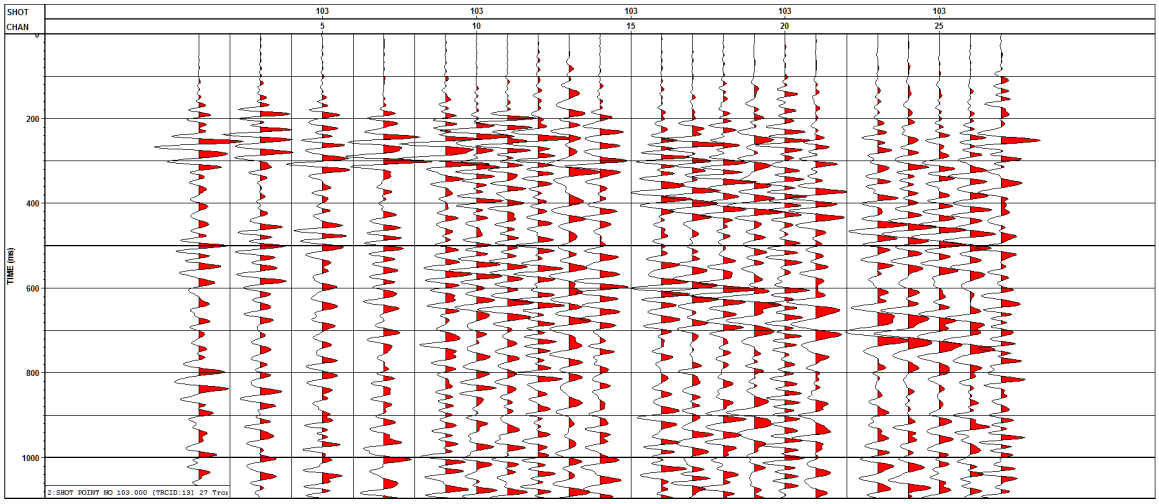

FIG. 21. Example of the Hmin component after first rotation (line 204, shot 103).

Second data rotation

The second step in the isolation of the downgoing P-wave events uses hodogram–based polarization on the Z and the Hmax data to output the Z' and Hmax' data. The rotation angles used for the polarization are found using a hodogram analysis of the Z and Hmax input data (Hinds et. al., 1996).

The rotation angle yield from the second hodogram analysis for the shots 1, 20 and 30 were compared with the incidence angle calculated with a ray tracing model in MATLAB. In this case, we define the incident angle as the angle of a ray-path with respect to the horizontal, as we are interested in a vertical interface since we are analyzing VSP data, therefore, the direction perpendicular to the interface is horizontal. A velocity model was computed using the sonic log from the 10-22 well. Since the first measurement of the sonic log was at approximately 222 m depth, a constant velocity layer was placed between the surface and that depth. The velocity used for the constant layer was the replacement velocity used for the shot statics (2600 m/s). Once the velocity model was created, a

raytracing function was used to compute the rays of the direct waves from a shot on surface with an offset of 400 m to all the receivers in the borehole. The ray parameter p was obtained as an output of the raytracing function, and it was used to calculate the incident angle. The raytracing model and the angles of the 400 m offset shot obtained are presented in Figure 22 and Figure 23 respectively.

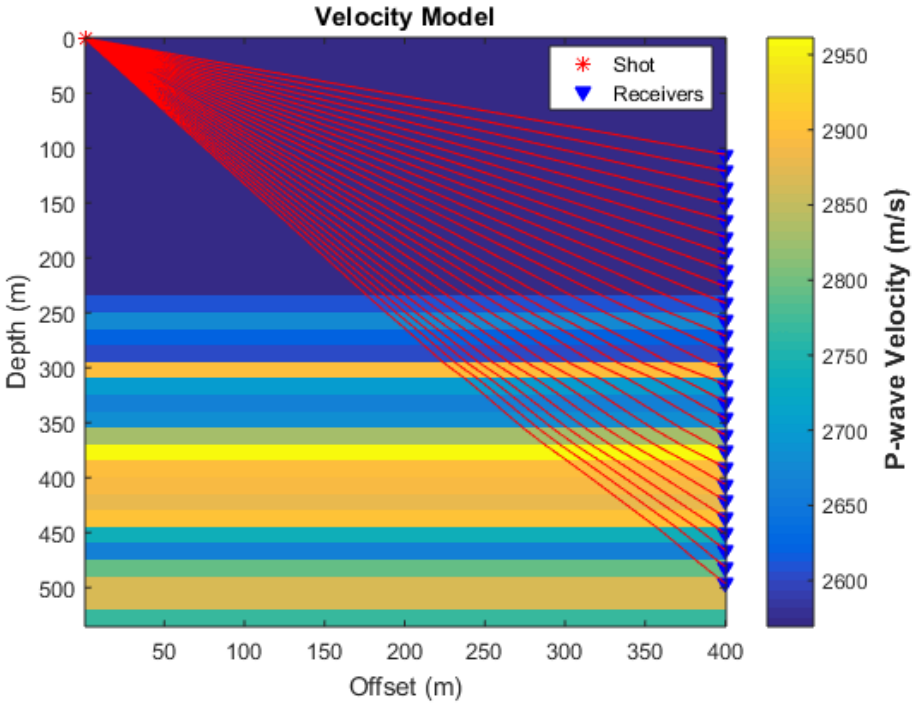

FIG. 22. Ray-tracing velocity model for a source on surface with an offset of 400m.

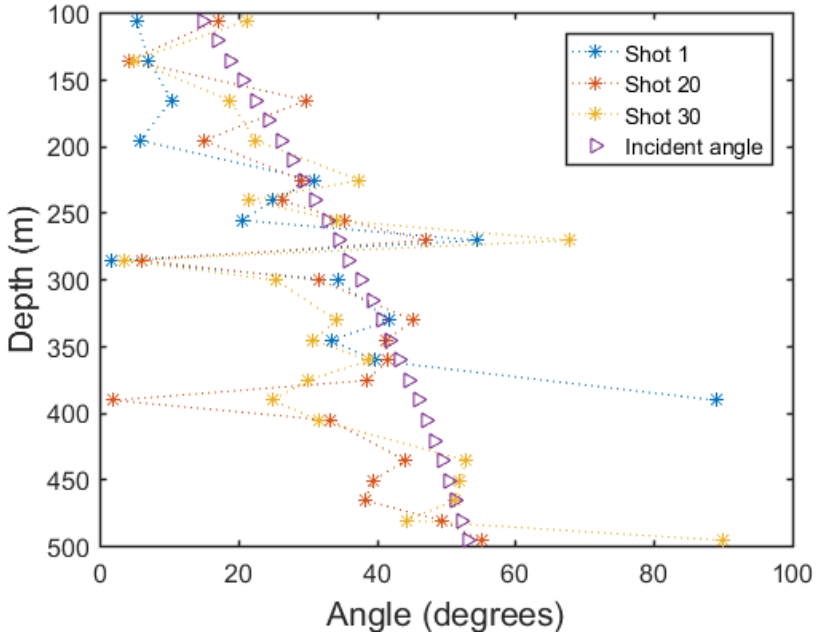

FIG. 23. Incident angle obtained from the ray-tracing velocity model (purple) and second rotation angles obtained for the shots 1, 20 and 30 using hodogram analysis.

A good relation is noticeable in Figure 23 between the incident angle obtained from the ray-tracing velocity map and the second rotation angles obtained from the hodogram analysis for the shots 1, 20 and 30. Nevertheless, there are some outliers in the rotation angles that are associated with the receivers at 286, 391 and 496 meters depth. As a future recommendation, a quality control analysis should be applied to the receivers since the outliers on Figure 16 are also associated to these receivers. Figures 24 and 25 shows an example of the data after the second rotation. Figure 24 represents the Hmax' component and Figure 25 represents the Z' component. From the results of the two rotations, we obtain the radial (Hmax'), transverse (Hmin) and vertical (Z) components of the data needed in order to continue the processing flow.

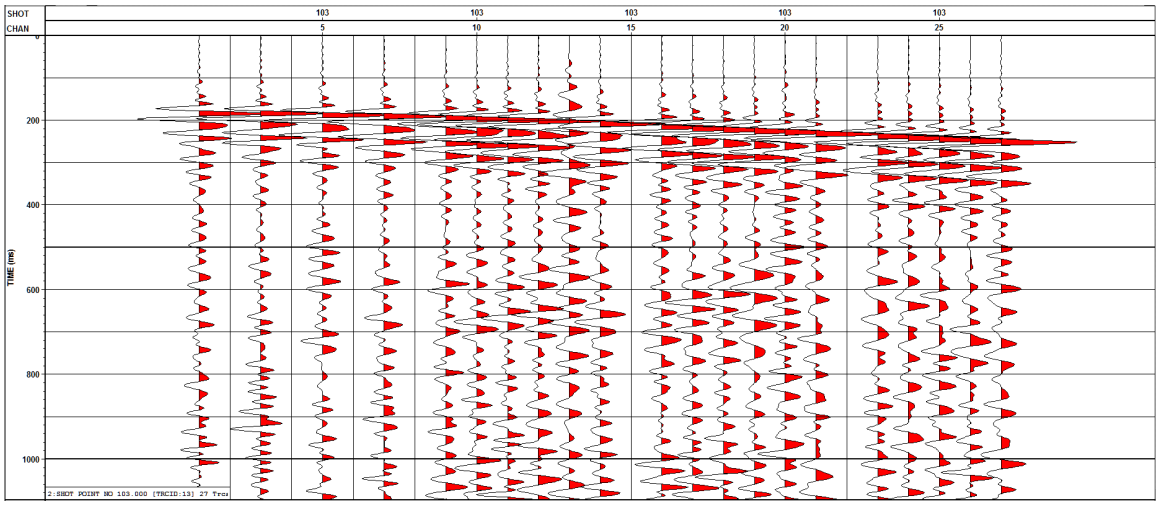

FIG. 24. Example of the Hmax' component after second rotation (line 204, shot 103).

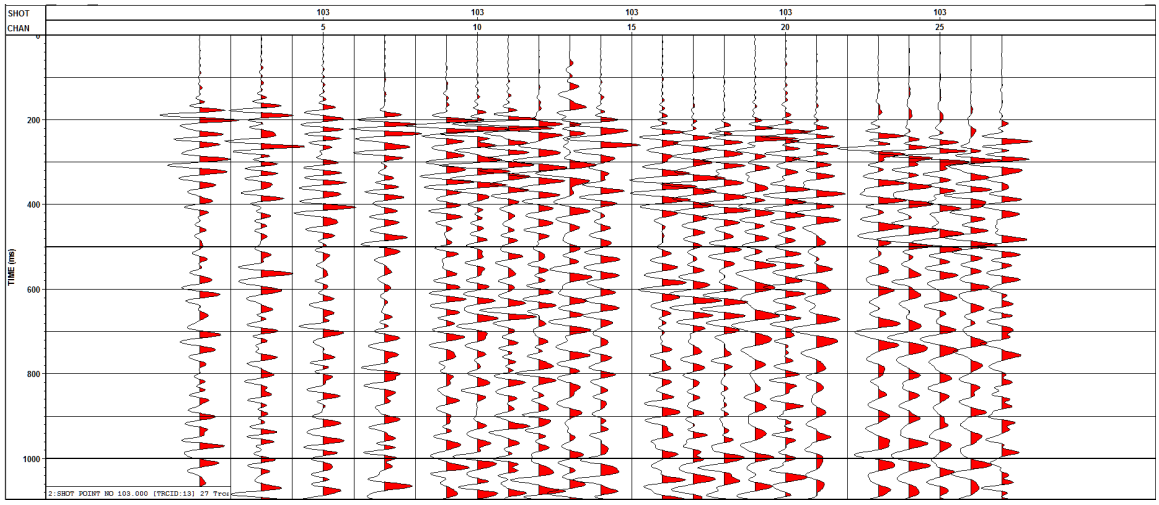

FIG. 25. Example of the Z' component after second rotation (line 204, shot 103).

CONCLUSIONS

The VSP azimuthal analysis was performed by studying the velocity changes in the first arrivals. This was done with the first break traveltime variation in respect to the azimuth of every receiver, and it showed good precision in all the points of the plot. After the static corrections and a median filter were applied, a smoother trend was observed. A sinusoidal trend is noticeable for the traveltime variation, which is indicative of azimuthal anisotropy (HTI). The fast direction shown is to the NE. With the traveltime and velocity residual calculation we were able to estimate an approximate value for epsilon equal to 0.02, indicative of weak anisotropy.

In the first step of processing, the rotation of the horizontal components H1 and H2 to Hmax and Hmin showed accurate results obtained with VISTA and MATLAB. After obtaining the rotation angle and comparing it in three different shots, the receivers showed a similar orientation with small variations that needs further analysis. However, quality control of the data would be recommended.

For the second data rotation, the incidence angle was calculated with two methods; the hodogram analysis and a ray-tracing velocity model. Both methods yield similar results, although there are several outliers in the hodogram results that needs further analysis. And as expected, the incidence angle tends to increase with depth.

FUTURE WORK

These achievements provide an opportunity to attempt further azimuthal analysis and the culmination of the processing flow for the walk-away VSP data and the walk-around VSP data in order to obtain imaging results.

Estimate the anisotropy parameters using a relation between the residual functions applied to the data and weak anisotropy approximations (WAA), introduced for example by Thomsen (1986), and Alkhalifah-Tsvankin (1995).

Develop a velocity model using the software NORSAR-2D Ray Modelling package would be useful to obtain the incidence angles and compare the results to those presented in this paper. Also, the use of synthetic data would be beneficial to compare results and get a better understanding of the area of study and what one would expect to find.

ACKNOWLEDGEMENTS

We would like to thank CREWES sponsors and NSERC (Natural Science and Engineering Research Council of Canada) support through the grant CRDPJ 461179-13. We also thank the Containment and Monitoring Institute (CaMI) and the Microseismic Industry Consortium for the opportunity to develop this research. Further thanks to Dr. Helen Isaac, Michelle Montano and Raul Cova for their guidance and discussions during this research.

REFERENCES

Lawton D., Bertram M., Bertram K., Hall K., and Isaac J. H., 2014. A 3C-3D seismic survey at a new field research station near Brooks, Alberta. CREWES Research Report, **26**-48.

Hardage, B.A. 2000. Vertical Seismic Profiling—Principles, third updated and revised edition. Pergamon.

Hinds R., Anderson N. and Kuzmiski R., 1996, VSP Interpretive Processing: Theory and Practice. *Open File Publications No.3.* Society of Exploration Geophysicists.

Evans J., Martinez P. A. and Jones M., 2010. Fundamentals of Borehole Seismic Technology. Schlumberger.

Lui E. and Martinez A., 2008. Seismic Fracture Characterization, Concepts and Practical applications. EAGE Education Tour Series.

Hall K., Isaac J. H., Wong J., Bertram K., Bertram M., Lawton D., Xuewei Bao, and David W.S. Eaton, 2015. Initial 3C-2D surface seismic and walkaway VSP results from the 2015 Brooks SuperCable experiment. CREWES Research Report, **27**-23.

Horne S., Slater C., Malek S., Hill A. and Wijnands F., 2000. Walkaround VSPs for fractured reservoir characterization. SEG Technical Program Expanded Abstracts, 1401-1404.

Thomsen L., 1986. Weak elastic anisotropy. GEOPHYSICS, Vol. 51, No. 10.

Alkhalifah T. and Tsvankin I., 1995. Velocity analysis for transversely isotropic media. GEOPHYSICS, Vol. 60, No. 5.